Journal of Experimental Marine Biology and Ecology 481 (2016) 9–14

Contents lists available at ScienceDirect

Journal of Experimental Marine Biology and Ecology

journal homepage: www.elsevier.com/locate/jembe

# $CO_2$-dependent carbon isotope fractionation in dinoflagellates relates to their inorganic carbon fluxes

Mirja Hoins [a,b,*], Tim Eberlein [b], Dedmer B. Van de Waal [c], Appy Sluijs [a], Gert-Jan Reichart [a,d], Björn Rost [b]

[a] Department of Earth Sciences, Faculty of Geosciences, Utrecht University, Budapestlaan 4, 3584 CD Utrecht, The Netherlands
[b] Marine Biogeosciences, Alfred Wegener Institute, Helmholtz Centre for Polar- and Marine Research, Am Handelshafen 12, 27570 Bremerhaven, Germany
[c] Department of Aquatic Ecology, Netherlands Institute of Ecology (NIOO-KNAW), Droevendaalsesteeg 10, 6708 PB Wageningen, The Netherlands
[d] Royal Netherlands Institute for Sea Research (NIOZ), Landsdiep 4, 1797 SZ 't Horntje, Texel, The Netherlands

ARTICLE INFO

*Article history:*
Received 12 September 2015
Received in revised form 3 April 2016
Accepted 4 April 2016
Available online 30 April 2016

*Keywords:*
CCM
$CO_2$ uptake
$HCO_3^-$ uptake
Leakage

ABSTRACT

Carbon isotope fractionation ($\varepsilon_p$) between the inorganic carbon source and organic matter has been proposed to be a function of $pCO_2$. To understand the $CO_2$-dependency of $\varepsilon_p$ and species-specific differences therein, inorganic carbon fluxes in the four dinoflagellate species *Alexandrium fundyense, Scrippsiella trochoidea, Gonyaulax spinifera* and *Protoceratium reticulatum* have been measured by means of membrane-inlet mass spectrometry. In-vivo assays were carried out at different $CO_2$ concentrations, representing a range of $pCO_2$ from 180 to 1200 μatm. The relative bicarbonate contribution (i.e. the ratio of bicarbonate uptake to total inorganic carbon uptake) and leakage (i.e. the ratio of $CO_2$ efflux to total inorganic carbon uptake) varied from 0.2 to 0.5 and 0.4 to 0.7, respectively, and differed significantly between species. These ratios were fed into a single-compartment model, and $\varepsilon_p$ values were calculated and compared to carbon isotope fractionation measured under the same conditions. For all investigated species, modeled and measured $\varepsilon_p$ values were comparable (*A. fundyense, S. trochoidea, P. reticulatum*) and/or showed similar trends with $pCO_2$ (*A. fundyense, G. spinifera, P. reticulatum*). Offsets are attributed to biases in inorganic flux measurements, an overestimated fractionation factor for the $CO_2$-fixing enzyme RubisCO, or the fact that intracellular inorganic carbon fluxes were not taken into account in the model. This study demonstrates that $CO_2$-dependency in $\varepsilon_p$ can largely be explained by the inorganic carbon fluxes of the individual dinoflagellates.



## 1. Introduction

During photosynthetic carbon fixation, the lighter carbon isotope $^{12}C$ is preferred over the heavier carbon isotope $^{13}C$, thereby causing carbon isotope fractionation ($\varepsilon_p$) between the inorganic carbon ($C_i$) source and the organic carbon. Values for $\varepsilon_p$ of marine phytoplankton have been shown to be $CO_2$-sensitive (e.g. Degens et al., 1968), and thus were discussed to serve as a proxy for past $CO_2$ concentrations (Jasper and Hayes, 1990; Pagani, 2014; Van de Waal et al., 2013; Hoins et al., 2015). Large species-specific differences in $\varepsilon_p$ have been described, which are yet poorly understood (e.g. Hinga et al., 1994; Burkhardt et al., 1999). Moreover, irrespective of the phytoplankton species investigated, most of these studies have solely described the relationship between $\varepsilon_p$ and $CO_2$, and only few have investigated the underlying physiological processes. Such mechanistic understanding is, however, needed to identify the reasons of the $CO_2$-dependency of $\varepsilon_p$.

Carbon isotope fractionation of phytoplankton is primarily driven by the enzyme ribulose-1,5-bisphosphate Carboxylase/Oxygenase (RubisCO), which is responsible for the fixation of $CO_2$ into organic compounds. The intrinsic fractionation associated with RubisCO ($\varepsilon_f$) has been estimated to range between ~22 and 30‰ (e.g. Roeske and O'Leary, 1984; Guy et al., 1993; Scott et al., 2007), even though a recent study obtained values as low as 11‰ for the RubisCO of the coccolithophore *Emiliania huxleyi* (Boller et al., 2011). While RubisCO principally sets the upper limit of fractionation, other processes strongly determine the degree to which RubisCO can express its fractionation (Sharkey and Berry, 1985; Burkhardt et al., 1999; Rost et al., 2002). First, there is leakage, i.e. the amount of $CO_2$ diffusing out of the cell in relation to $C_i$ uptake. With higher leakage, the intracellular $C_i$ pool is 'refreshed', thereby preventing accumulation of $^{13}C$ and allowing RubisCO to approach its upper fractionation values. Second, the relative

*Abbreviations:* $C_i$, inorganic carbon; CCM, $CO_2$-concentrating mechanism; Chl-*a*, Chlorophyll-*a*; $\varepsilon_p$, carbon isotope fractionation; $\varepsilon_{p\text{-meas}}$, measured carbon isotope fractionation; $\varepsilon_{p\text{-mod}}$, modeled carbon isotope fractionation; $\varepsilon_s$, equilibrium fractionation between $CO_2$ and $HCO_3^-$; $\varepsilon_f$, kinetic fractionation associated with the $CO_2$ fixation of RubisCO; $L_{CO2}$, ratio of $CO_2$ efflux relative to total $C_i$ uptake; DIC, dissolved inorganic carbon; $HCO_3^-$, bicarbonate; $R_{HCO3}$, ratio of $HCO_3^-$ to total $C_i$ uptake; RubisCO, ribulose-1,5-bisphosphate Carboxylase/Oxygenase; CA, carbonic anhydrase; TA, total alkalinity.

* Corresponding author at: Department of Earth Sciences, Faculty of Geosciences, Utrecht University, Budapestlaan 4, 3584 CD Utrecht, The Netherlands.
*E-mail addresses:* mhoins@awi.de (M. Hoins), tim.eberlein@awi.de (T. Eberlein), D.vandeWaal@nioo.knaw.nl (D.B. Van de Waal), a.sluijs@uu.nl (A. Sluijs), g.j.reichart@uu.nl (G.-J. Reichart), bjoern.rost@awi.de (B. Rost).

http://dx.doi.org/10.1016/j.jembe.2016.04.001

contribution of bicarbonate ($HCO_3^-$) to total $C_i$ uptake plays a role, as $HCO_3^-$ is enriched in $^{13}C$ by ~10‰ relative to $CO_2$ (Mook et al., 1974). An increasing $HCO_3^-$ contribution thus lowers $\varepsilon_p$. The enzyme carbonic anhydrase (CA), which accelerates the otherwise slow interconversion between $CO_2$ and $HCO_3^-$, can also influence $\varepsilon_p$ under certain conditions, e.g. by influencing leakage as well as the relative $HCO_3^-$ contribution. All these processes play a role in the $CO_2$-concentrating mechanisms (CCMs) of phytoplankton. Assessing the mode of CCMs may therefore help to understand the reasons for $CO_2$-dependent changes in $\varepsilon_p$ and species-specific differences therein.

Dinoflagellates are cosmopolitan unicellular algae that occur in many different environments, including eutrophic coastal regions and oligotrophic open oceans. In this study, we investigated whether the $CO_2$-dependency of $\varepsilon_p$, which was found in the dinoflagellate species *Alexandrium fundyense, Gonyaulax spinifera*, *Protoceratium reticulatum* and *Scrippsiella trochoidea* (Burkhardt et al., 1999; Hoins et al., 2015), can be explained by changes in their $C_i$ fluxes. Characteristics of CCMs in the tested species, including their CA activities and $C_i$ fluxes, were measured by means of membrane-inlet mass spectrometry (MIMS). Results were fed into a single-compartment model that considers cellular leakage, the relative $HCO_3^-$ contribution as well as the carbon isotope fractionation of RubisCO (Sharkey and Berry, 1985; Burkhardt et al., 1999). The calculated carbon fractionation ($\varepsilon_{p\text{-}mod}$) was then compared to the measured carbon fractionation ($\varepsilon_{p\text{-}meas}$).

## 2. Material and methods

### 2.1. Incubations

Cultures of the dinoflagellate species *A. fundyense* (formerly *Alexandrium tamarense* strain Alex5; John et al., 2014), *S. trochoidea* (strain GeoB267; culture collection of the University of Bremen), *G. spinifera* (strain CCMP 409) and *P. reticulatum* (strain CCMP 1889) were grown in 0.2 μm filtered North Sea water (salinity 34), which was enriched with 100 μmol $L^{-1}$ nitrate and 6.25 μmol $L^{-1}$ phosphate. Metals and vitamins were added according to f/2 medium (Guillard and Ryther, 1962), except for $FeCl_3$ (1.9 μmol $L^{-1}$), $H_2SeO_3$ (10 nmol $L^{-1}$) and $NiCl_2$ (6.3 nmol $L^{-1}$) that were added according to K medium (Keller et al., 1987). Each of the strains was grown in 2.4 L air-tight borosilicate bottles at 15 °C and 250 ± 25 μmol photons $m^{-2}$ $s^{-1}$ at a 16:8 h light:dark cycle. Bottles were placed on roller tables in order to avoid sedimentation.

Dissolved $CO_2$ concentrations ranged from ~5–50 μmol $L^{-1}$ and were reached by pre-aerating culture medium with air containing 180, 380, 800 and 1200 μatm $pCO_2$. The carbonate chemistry was calculated based on pH and total alkalinity (TA), using the program CO2sys (Pierrot et al., 2006). pH values were measured using a WTW 3110 pH meter equipped with a SenTix 41 Plus pH electrode (WTW, Weilheim, Germany), which was calibrated prior to measurements to the National Bureau of Standards (NBS) scale. An automated TitroLine burette system (SI Analytics, Mainz, Germany) was used to determine TA. Dissolved inorganic carbon (DIC) was determined colorimetrically using a QuAAtro autoanalyser (Seal Analytical, Mequon, USA). For more details on the carbonate chemistry in the acclimations, please refer to Eberlein et al. (2014) for *A. fundyense* and *S. trochoidea* and to Hoins et al. (2015) for *G. spinifera* and *P. reticulatum*.

To determine $\varepsilon_p$ values, the isotopic composition of the organic material was measured using an Automated Nitrogen Carbon Analyser mass spectrometer (ANCA-SL 20–20, SerCon Ltd., Crewe, UK), and the isotopic composition of the DIC in growth medium was measured using a GasBench-II coupled to a Thermo Delta-V advantage isotope ratio mass spectrometer (see Hoins et al., 2015 for details on isotope analysis). Prior to assays, cells were acclimated to the different $CO_2$ concentrations for at least 7 generations (i.e. >21 days). To prevent changes in the carbonate chemistry, i.e. keeping drawdown of DIC <3%, incubations were terminated at low cell densities (<400 cells $mL^{-1}$).

### 2.2. MIMS assays

A custom-made membrane-inlet mass spectrometer (MIMS; Isoprime, GV Instruments, Manchester, UK; see Rost et al., 2007 for details) was used to determine CA activities and $C_i$ fluxes of *A. fundyense* and *S. trochoidea* acclimated to four different $pCO_2$ (i.e. 180, 380, 800 and 1200 μatm; Eberlein et al., 2014), and of *G. spinifera* and *P. reticulatum* acclimated to a low and high $pCO_2$ (i.e. 180 and 800 μatm). Assays were performed in an 8 mL temperature-controlled cuvette, equipped with a stirrer. Assay tests over ~1 h confirmed that conditions during the assay do not cause physiological stress (i.e. no decline in $O_2$ production rates), and subsequent microscopic inspection did not reveal any visual effects on cell morphologies. Prior to the measurements, acclimated cells were concentrated using a 10 μm membrane filter (Millipore, Billerica, MA) by gentle vacuum filtration (<200 mbar) and stepwise transferred into $C_i$-free medium buffered with a 4-(2-hydroxylethyl)-1-piperazine-ethanesulfonic acid (50 $mmol^{-1}$ HEPES) solution at 15 ± 0.3 °C and a pH of 8.0 ± 0.1. Chlorophyll *a* (Chl-*a*) concentrations were determined fluorometrically by using a TD-700 Fluorometer (Turner Designs, Sunnyvale, CA, USA) and ranged between 0.15 and 1.70 μg $mL^{-1}$ during the assays.

To quantify activities of extracellular CA (eCA), the $^{18}O$ depletion rate of doubly labeled $^{13}C^{18}O_2$ in seawater was determined by measuring the transient changes in $^{13}C^{18}O^{18}O$ (m/z = 49), $^{13}C^{18}O^{16}O$ (m/z = 47) and $^{13}C^{16}O^{16}O$ (m/z = 45) in the dark, following the approach of Silvermann (1982). If cells possess eCA, exchange rates of $^{18}O$ are accelerated relative to the spontaneous rate. To monitor the spontaneous rate, $NaH^{13}C^{18}O_3$ label was injected to the cuvette, waiting until the m/z = 49 signal reached a steady-state decline. This rate was then compared to the steady-state decline after cells were added. Following Badger and Price (1989), eCA activity is expressed as percentage decrease in $^{18}O$-atom fraction upon the addition of cells, normalized to Chl-*a*. Consequently, 100 units (U) correspond to a doubling in the rate of interconversion between $CO_2$ and $HCO_3^-$ per μg Chl-*a*.

Photosynthetic $O_2$ and $C_i$ fluxes were determined following Badger et al. (1994). Making use of the chemical disequilibrium, this approach estimates $CO_2$ and $HCO_3^-$ fluxes during steady-state photosynthesis. It is based on the simultaneous measurements of $O_2$ and $CO_2$ concentrations during consecutive light and dark intervals with increasing amounts of DIC. Oxygen fluxes in the dark and light are converted into $C_i$ fluxes by applying a respiratory quotient of 1.0 and a photosynthetic quotient of 1.1 (Burkhardt et al., 2001; Rost et al., 2003). The light intensity in the cuvette was adjusted to the acclimation conditions (i.e. 250 ± 25 μmol photons $m^{-2}$ $s^{-1}$). Net $CO_2$ uptake was calculated from the steady-state decline in $CO_2$ concentration at the end of the light period, corrected for the interconversion between $CO_2$ and $HCO_3^-$. The uptake of $HCO_3^-$ was calculated by subtracting net $CO_2$ uptake from net $C_i$ uptake, and the $CO_2$ efflux from the cells was estimated from the initial slope after turning off the light. Rate constants $k_1$ and $k_2$ were determined based on temperature, salinity and pH (Zeebe and Wolf-Gladrow, 2001; Schulz et al., 2006), yielding mean values of 0.9241 (±0.0506) $min^{-1}$ and 0.0085 (±0.0008) $min^{-1}$, respectively. To eliminate any eCA activity, a prerequisite to apply the rate constants, we added dextran-bound sulfonamide (DBS; 50 μmol $L^{-1}$) to the cuvette. For more details on the calculations, please refer to Badger et al. (1994) and Schulz et al. (2007).

### 2.3. Single-compartment model

To calculate $\varepsilon_{p\text{-}mod}$, results for the relative $HCO_3^-$ contribution and leakage were fed into a single-compartment model after Sharkey and

Berry (1985) and Burkhardt et al. (1999):

$$\varepsilon_{p-\,mod} = R_{HCO3} \times \varepsilon_s + L_{CO2} \times \varepsilon_f \quad (1)$$

where $R_{HCO3}$ represents the ratio of $HCO_3^-$ to total $C_i$ uptake, $\varepsilon_s$ the equilibrium fractionation between $CO_2$ and $HCO_3^-$ (−10‰; Mook et al., 1974), $L_{CO2}$ the ratio of $CO_2$ efflux relative to total $C_i$ uptake, and $\varepsilon_f$ the kinetic fractionation associated with the $CO_2$ fixation of RubisCO, which was here assumed to be 28‰ after Raven and Johnston (1991).

### 2.4. Statistical analysis

Shapiro–Wilk tests confirmed normality of the data. Significant differences between $CO_2$ treatments were confirmed by a one-way ANOVA followed by post hoc comparison of the means using the Tukey HSD ($\alpha = 0.05$; Table 1).

## 3. Results

### 3.1. CA activity

In *A. fundyense* and *P. reticulatum*, eCA activities were low with maximum activities of 156 U (μg Chl-*a*)$^{-1}$ and 44 U (μg Chl-*a*)$^{-1}$, respectively. In *S. trochoidea* and *G. spinifera*, eCA activities were comparably high with up to 1600 U (μg Chl-*a*)$^{-1}$ and 1100 U (μg Chl-*a*)$^{-1}$, respectively. In neither of the species, eCA activities were responding to changes in $pCO_2$. Please note that for *G. spinifera* and *P. reticulatum* no statistics could be applied due to the lack of replication.

### 3.2. $HCO_3^-$ contribution and leakage

Relative $HCO_3^-$ contribution was around 0.2 in *A. fundyense* and *G. spinifera* (Figs. 1A and 3A; Table 1), whereas *S. trochoidea* and *P. reticulatum* showed higher values of ~0.5 (Figs. 2A and 4A; Table 1). In other words, in *A. fundyense* and *G. spinifera* approximately 80% of the $C_i$ taken up is in the form of $CO_2$, whereas in *S. trochoidea* and *P. reticulatum* this was 50%. There was a significant decrease in $HCO_3^-$ contribution with increasing $CO_2$ concentration in *S. trochoidea*, while no such $CO_2$-dependency was observed in any of the other tested species. Leakage differed significantly between the tested species, with values of up to 0.7 at 800 μatm $pCO_2$ in *G. spinifera* (Fig. 3A; Table 1) and lowest average values of ~0.5 in *S. trochoidea* and *P. reticulatum*,

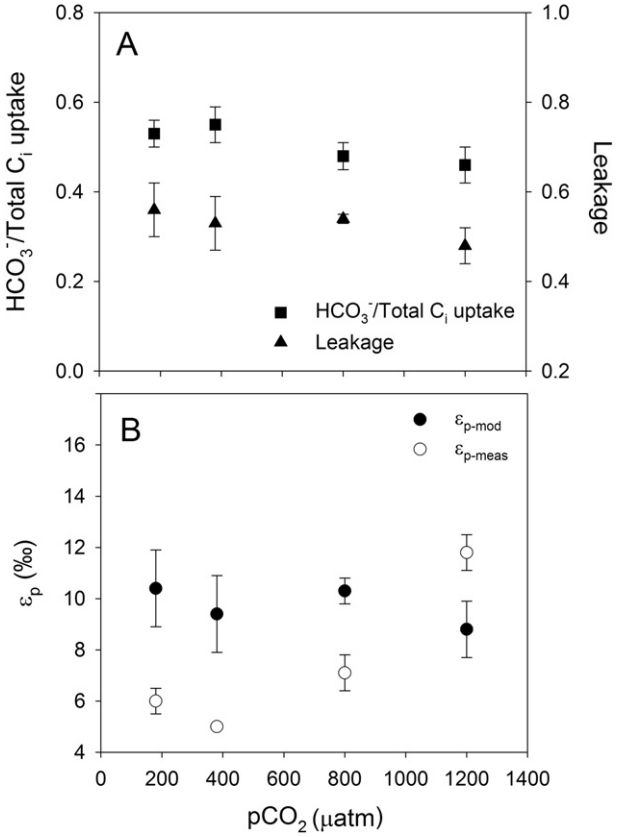


**Fig. 1.** Relative $HCO_3^-$ contribution, leakage and $\varepsilon_{p\text{-}mod}$ and $\varepsilon_{p\text{-}meas}$ in *A. fundyense*. Each data point represents the mean ± standard deviation (n = 3).

**Table 1**
Experimental conditions in dilute batch culture incubations (see also Eberlein et al., 2014; Hoins et al., 2015): average $CO_2$ concentrations (μmol L$^{-1}$), total alkalinity (TA; μmol L$^{-1}$), dissolved inorganic carbon (DIC; μmol L$^{-1}$) and pH (NBS scale). $HCO_3^-$ contribution, leakage, modeled carbon isotope fractionation ($\varepsilon_{p\text{-}mod}$) and measured carbon isotope fractionation ($\varepsilon_{p\text{-}meas}$) was derived under the same conditions.

| $pCO_2$ μatm | $CO_2$ μmol L$^{-1}$ | TA μmol L$^{-1}$ | DIC μmol L$^{-1}$ | pH NBS | $HCO_3^-$ contribution | Leakage | $\varepsilon_{p\text{-}mod}$ ‰ | $\varepsilon_{p\text{-}meas}$ ‰ |
|---|---|---|---|---|---|---|---|---|
| *A. fundyense* | | | | | | | | |
| 180 | 5.9 ± 0.9$^a$ | 2434 ± 3 | 1992 ± 10$^a$ | 8.50 ± 0.06$^a$ | 0.22 ± 0.03 | 0.44 ± 0.01$^a$ | 10.1 ± 0.2$^a$ | 9.0 ± 0.3$^a$ |
| 380 | 11.5 ± 2.1$^b$ | 2439 ± 1 | 2117 ± 8$^b$ | 8.27 ± 0.07$^b$ | 0.24 ± 0.04 | 0.46 ± 0.02$^a$ | 10.6 ± 0.5$^a$ | 10.2 ± 0.5$^b$ |
| 800 | 25.9 ± 5.8$^c$ | 2434 ± 2 | 2245 ± 8$^c$ | 7.97 ± 0.10$^c$ | 0.24 ± 0.04 | 0.53 ± 0.02$^b$ | 12.6 ± 0.6$^b$ | 12.7 ± 0.4$^c$ |
| 1200 | 36.5 ± 9.3$^d$ | 2418 ± 1 | 2283 ± 5$^d$ | 7.83 ± 0.12$^d$ | 0.23 ± 0.08 | 0.63 ± 0.05$^c$ | 15.3 ± 0.8$^c$ | 12.1 ± 0.2$^c$ |
| *S. trochoidea* | | | | | | | | |
| 180 | 6.6 ± 0.2$^a$ | 2386 ± 1 | 1872 ± 2$^a$ | 8.45 ± 0.01$^a$ | 0.53 ± 0.03$^{a,b}$ | 0.56 ± 0.06 | 10.4 ± 1.5 | 6.0 ± 0.5$^{a,b}$ |
| 380 | 13.1 ± 0.5$^b$ | 2388 ± 2 | 2096 ± 3$^b$ | 8.21 ± 0.02$^b$ | 0.55 ± 0.04$^a$ | 0.53 ± 0.06 | 9.4 ± 1.5 | 5.0 ± 0.1$^a$ |
| 800 | 28.8 ± 2.0$^c$ | 2385 ± 1 | 2223 ± 3$^c$ | 7.91 ± 0.03$^c$ | 0.48 ± 0.03$^{b,c}$ | 0.54 ± 0.01 | 10.3 ± 0.5 | 7.1 ± 0.7$^b$ |
| 1200 | 41.5 ± 3.6$^d$ | 2386 ± 4 | 2268 ± 9$^d$ | 7.77 ± 0.04$^d$ | 0.46 ± 0.04$^c$ | 0.48 ± 0.04 | 8.8 ± 1.1 | 11.8 ± 0.7$^c$ |
| *G. spinifera* | | | | | | | | |
| 180 | 6.0 ± 1.1$^a$ | 2447 ± 5 | 1962 ± 15$^a$ | 8.50 ± 0.05$^a$ | 0.19 ± 0.11 | 0.61 ± 0.01 | 15.6 ± 0.9$^a$ | 7.8 ± 1.0$^a$ |
| 380 | 11.7 ± 2.5$^b$ | 2461 ± 12 | 2083 ± 1$^b$ | 8.27 ± 0.07$^b$ | – | – | – | 9.4 ± 0.4$^a$ |
| 800 | 27.9 ± 7.4$^c$ | 2475 ± 13 | 2224 ± 9$^c$ | 7.96 ± 0.10$^c$ | 0.19 ± 0.11 | 0.71 ± 0.01 | 18.6 ± 1.7$^b$ | 11.7 ± 0.7$^b$ |
| 1200 | 42.4 ± 7.9$^d$ | 2459 ± 4 | 2293 ± 5$^d$ | 7.78 ± 0.06$^d$ | – | – | – | 8.1 ± 0.5$^a$ |
| *P. reticulatum* | | | | | | | | |
| 180 | 7.1 ± 0.5$^a$ | 2460 ± 8 | 2002 ± 2$^a$ | 8.43 ± 0.04$^a$ | 0.44 ± 0.13 | 0.50 ± 0.06 | 9.58 ± 2.0 | 8.4 ± 1.8 |
| 380 | 13.9 ± 0.8$^b$ | 2455 ± 2 | 2121 ± 4$^b$ | 8.21 ± 0.02$^b$ | – | – | – | 8.4 ± 0.7 |
| 800 | 31.0 ± 4.7$^c$ | 2461 ± 12 | 2249 ± 23$^c$ | 7.88 ± 0.08$^c$ | 0.49 ± 0.19 | 0.48 ± 0.09 | 9.2 ± 1.9 | 8.6 ± 2.0 |
| 1200 | 45.2 ± 6.9$^d$ | 2473 ± 19 | 2288 ± 16$^d$ | 7.75 ± 0.05$^d$ | – | – | – | 9.9 ± 0.8 |

Values represent the mean of triplicate incubations (n = 3; ±SD). Superscript letters indicate significant differences between $pCO_2$ treatments ($P < 0.05$).

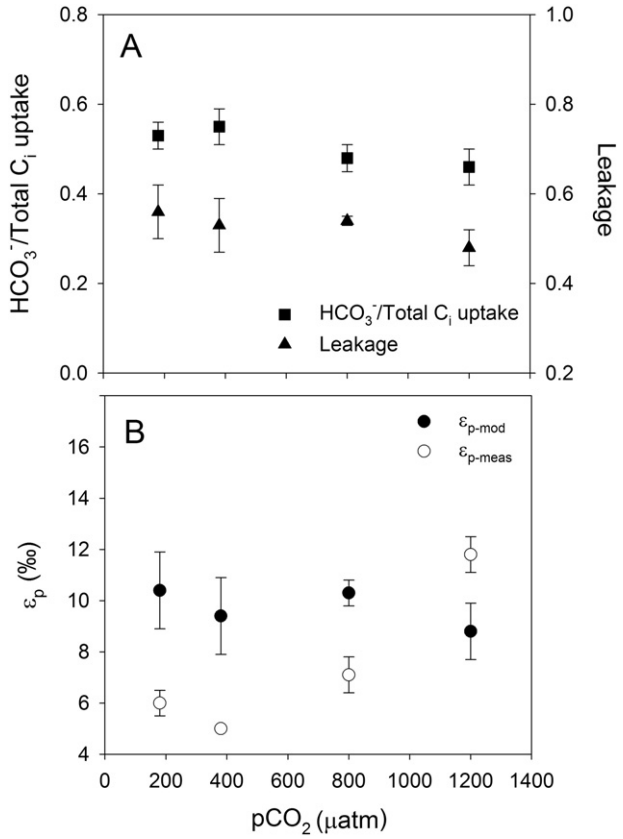


**Fig. 2.** A) Relative $HCO_3^-$ contribution, leakage and B) $\varepsilon_{p\text{-mod}}$ and $\varepsilon_{p\text{-meas}}$ in *S. trochoidea*. Each data point represents the mean ± standard deviation (n = 3).

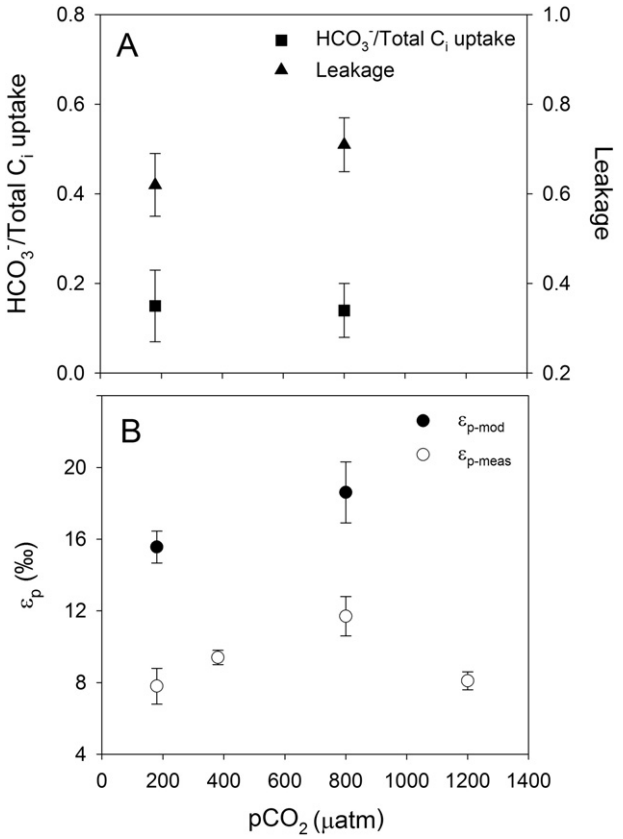


**Fig. 3.** A) Relative $HCO_3^-$ contribution, leakage and B) $\varepsilon_{p\text{-mod}}$ and $\varepsilon_{p\text{-meas}}$ in *G. spinifera*. Each data point represents the mean ± standard deviation (n = 3).

respectively (Figs. 2A and 4A; Table 1). Only in *A. fundyense*, leakage was significantly $CO_2$-dependent and increased from 0.44 to 0.63 (Fig. 1A; Table 1). For details on the kinetics of $O_2$, $CO_2$ and $HCO_3^-$ fluxes in *A. fundyense* and *S. trochoidea*, please refer to Eberlein et al. (2014).

### 3.3. $C_i$ flux based $\varepsilon_p$ calculations

Estimates for $\varepsilon_{p\text{-mod}}$ are in the same range as $\varepsilon_{p\text{-meas}}$ in *A. fundyense* and *P. reticulatum* (Figs. 1B and 4B; Table 1), while the model overestimated the fractionation by up to 5‰ and 8‰ in *S. trochoidea* and *G. spinifera*, respectively (Figs. 2B and 3B; Table 1). Except for *S. trochoidea*, $\varepsilon_{p\text{-mod}}$ generally matches trends observed in $\varepsilon_{p\text{-meas}}$. In *A. fundyense*, for instance, $\varepsilon_{p\text{-mod}}$ increased significantly from 10.1 to 15.3‰, thereby closely matching $\varepsilon_{p\text{-meas}}$ values (Fig. 1B; Table 1). Also in *G. spinifera*, $\varepsilon_{p\text{-mod}}$ matches trends observed in $\varepsilon_{p\text{-meas}}$, if the highest $pCO_2$ treatment of $\varepsilon_{p\text{-meas}}$ is excluded. In this treatment, carbon isotope fractionation dropped significantly, most likely due to 2.5-fold increased cellular carbon contents (see discussion in Hoins et al., 2015). In *S. trochoidea*, neither the relative $HCO_3^-$ contribution nor leakage showed a $CO_2$-dependency; hence $\varepsilon_{p\text{-mod}}$ did not match the increase in $\varepsilon_{p\text{-meas}}$ with increasing $CO_2$ concentration (Fig. 2B; Table 1).

## 4. Discussion

### 4.1. CA activity plays a minor role in $C_i$ fluxes

By expressing CA, many marine algae species accelerate the otherwise slow interconversion between $CO_2$ and $HCO_3^-$, thereby possibly facilitating the $C_i$ uptake and internal $C_i$ fluxes. In line with previous studies on dinoflagellates (Rost et al., 2006; Ratti et al., 2007), *A. fundyense* and *P. reticulatum* exhibit rather low eCA activities, even under low $CO_2$ concentrations. In view of this, eCA is not expected to significantly influence $C_i$ fluxes or $\varepsilon_p$ in these species. In *S. trochoidea* and *G. spinifera*, however, eCA activities were high at all tested $CO_2$ concentrations, comparable to values observed for temperate diatoms (Trimborn et al., 2009). Hence, the inhibition of eCA by the inhibitor DBS during the MIMS assay might have biased the $C_i$ fluxes, i.e. underestimated $CO_2$ uptake (Rost et al., 2003), thereby potentially causing an underestimation of $\varepsilon_p$. As these were the species for which the model overestimated $\varepsilon_p$ values, however, it can be concluded that eCA (and its inhibition by DBS during the $C_i$ flux measurements) did not influence the $C_i$ fluxes much.

### 4.2. Species-specific differences in $C_i$ fluxes

The $HCO_3^-$ contribution differed considerably between the tested species. While *A. fundyense* and *G. spinifera* showed a strong preference for $CO_2$, *S. trochoidea* and *P. reticulatum* used $CO_2$ and $HCO_3^-$ in equal proportions. The latter contradicts with the findings of an endpoint pH-drift experiment, suggesting that *P. reticulatum* is not able to efficiently use $HCO_3^-$ (Ratti et al., 2007). Testing other dinoflagellates with a modified pH-drift method, including the genus *Protoceratium*, demonstrated that the high pH itself can affect growth and thus interpretations about the used $C_i$ source based on pH-drift experiments must be considered with caution (Hansen et al., 2007). From an energetic point of view, high $CO_2$ usage would be of advantage as $CO_2$ can be taken up passively by diffusion, while $HCO_3^-$ is charged and thus has to be taken up by active uptake. And yet, the tested species covered a large part of their $C_i$ demand by $HCO_3^-$, as observed in *S. trochoidea* and *P. reticulatum* (Figs. 2A and 4A).

Similarly high $HCO_3^-$ contributions were observed for other dinoflagellate species (Rost et al., 2006) and cyanobacteria (Price et al., 2008; Kranz et al., 2011). This preference for $HCO_3^-$ has been associated with the very low $CO_2$-affinity of RubisCO type IB, which is expressed

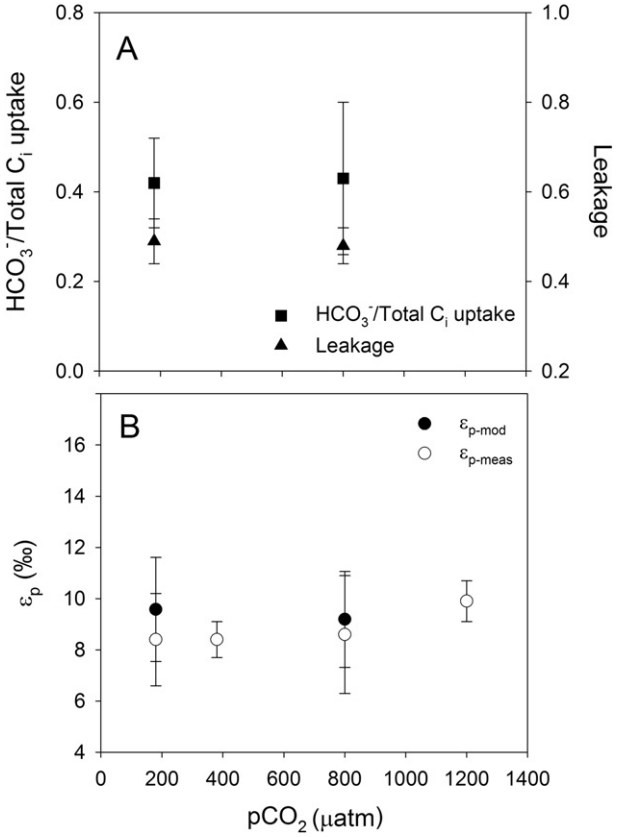


**Fig. 4.** A) Relative $HCO_3^-$ contribution, leakage and B) $\varepsilon_{p\text{-}mod}$ and $\varepsilon_{p\text{-}meas}$ in *P. reticulatum*. Each data point represents the mean ± standard deviation (n = 3).

in cyanobacteria, and RubisCO type II expressed in dinoflagellates (Badger et al., 1998; Whitney and Andrews, 1998). To compensate for this low affinity, high amounts of $C_i$ have to be accumulated, which in seawater can more easily be accomplished with the abundant $HCO_3^-$ ion rather than with $CO_2$. In addition, $HCO_3^-$ is about 1000-fold less permeable to lipid membranes than $CO_2$, making it the preferred $C_i$ form to be accumulated within the cell (Price et al., 2008). In the case where species covered the majority of their $C_i$ demand by $CO_2$, as observed in *A. fundyense* and *G. spinifera* (Figs. 1A and 3A), one could therefore speculate about chloroplast-based $C_i$ accumulation rather than pumping of $HCO_3^-$ at the cell wall (Badger et al., 1998). The observed differences in the preferred $C_i$ source and likely consequences for internal $C_i$ fluxes may also affect the overall leakage of cells.

Also leakage differed considerably among the species. *A. fundyense* showed a relatively low leakage of 0.44 at 180 µatm $pCO_2$, which increased to 0.63 at 1200 µatm $pCO_2$. Leakage in *G. spinifera* varied between 0.60 at 180 µatm $pCO_2$ and 0.70 at 800 µatm $pCO_2$. Leakage estimates in *S. trochoidea* and *P. reticulatum* were lower with ~0.50 and remained constant over the applied range of $pCO_2$. These differences may be caused by different membrane permeabilities, which again potentially relate to the preferred $C_i$ source. In fact, *A. fundyense* and *G. spinifera* both preferred $CO_2$ over $HCO_3^-$ and likewise showed the highest degrees of leakage, thereby suggesting highly permeable membranes with respect to $CO_2$. In these species, also $CO_2$-related changes in the membrane permeability are indicated as they show significantly increased leakage under higher $pCO_2$ (see also Eberlein et al., 2014 for *A. fundyense*, formerly *A. tamarense*).

### 4.3. Patterns in carbon isotope fractionation can be explained by $C_i$ fluxes

Using results for $HCO_3^-$ contribution and leakage obtained in this study, carbon isotope fractionation was calculated and compared to previous measurements (Figs. 1B–4B; see also Hoins et al., 2015). Generally, there is a good agreement as $\varepsilon_{p\text{-}mod}$ and $\varepsilon_{p\text{-}meas}$ values were in the same range (*A. fundyense, S. trochoidea, P. reticulatum*) and/or followed the same trend (*A. fundyense, G. spinifera, P. reticulatum*; Figs. 1B-4B). Despite the overall agreement between flux-based estimates and directly measured carbon isotope fractionation, $\varepsilon_{p\text{-}mod}$ was overestimated in *S. trochoidea* and *G. spinifera*. Such offsets could principally be attributed to biases in the $C_i$ flux measurements, i.e. uncertainties in the estimation of $HCO_3^-$ contribution and/or leakage. It has been argued, however, that the MIMS approach tends to overestimate the $HCO_3^-$ contribution (due to the constant pH of 8.0 during the assay, see Burkhardt et al., 2001), and rather underestimates cellular leakage (due to fact that $CO_2$ fixation does not cease instantly upon darkening, see Badger et al., 1994). Hence, by correcting for these potential biases, i.e. assuming slightly lower $HCO_3^-$ contribution and higher leakage values, we would actually overestimate the fractionation even more for *S. trochoidea* and *G. spinifera*.

An alternative explanation for the overestimation by the model may be attributed to the fractionation factor of RubisCO, which we assumed to be 28‰ (Raven and Johnston, 1991). Recent studies have found lower values, even as low as 11‰ as in the case of the coccolithophore *Emiliania huxleyi* (Boller et al., 2011). Even though there are no indications for such low fractionation values in the highly conserved type II RubisCO, a lower fractionation would bring modeled and measured $\varepsilon_p$ values closer in *S. trochoidea* and *G. spinifera*. In *A. fundyense* and *P. reticulatum*, however, it would lead to underestimated $\varepsilon_{p\text{-}mod}$. Hence, we would refrain from assuming much lower fractionation values for RubisCO type II in dinoflagellates in our calculations. Lastly, the fact that internal $C_i$ fluxes were not taken into account might have also contributed to the offsets between $\varepsilon_{p\text{-}mod}$ and $\varepsilon_{p\text{-}meas}$. Models that incorporate internal $C_i$ cycling have, however, caused even higher $\varepsilon_{p\text{-}mod}$, as these processes work against the $^{13}C$ accumulation within the chloroplasts (Cassar et al., 2006; Schulz et al., 2007) or the carboxysome (Eichner et al., 2015). Therefore, although the values and trends in carbon isotope fractionation are relatively well understood based on our physiological experiments, differences between theory and measurements are at present not fully resolved.

## 5. Conclusions

Our study demonstrates that carbon isotope fractionation in dinoflagellates can, to a large degree, be explained by considering their $C_i$ fluxes. Relative $HCO_3^-$ contribution and/or leakage were $CO_2$-dependent in *A. fundyense, S. trochoidea* and *G. spinifera*, which in turn can explain the $CO_2$-dependency of their $\varepsilon_p$ observed in previous studies (Hoins et al., 2015). To further advance our understanding of the $\varepsilon_p$ patterns in dinoflagellates, $C_i$ fluxes measurements should be performed at in situ pH (Kottmeier et al., 2014, 2016) and ideally differentiate between $^{13}C$ and $^{12}C$ fluxes (McNevin et al., 2006).

## Acknowledgments

This research was funded through the Darwin Centre for Biogeosciences Grant 3021, awarded to GJR and AS, and the European Research Council under the Seventh Framework Program of the European Community through ERC Starting Grants #259627 to AS and #205150 to BR. DBvdW and BR thank BIOACID, financed by the German Ministry of Education and Research. This work was carried out under the program of the Netherlands Earth System Science Centre (NESSC). We thank Urban Tillmann (Alfred Wegener Institute) and Karin Zonneveld (Marum, Bremen University) for providing the dinoflagellate species *Alexandrium fundyense* Alex5 and *Scrippsiella trochoidea* GeoB267, respectively, and Ulrike Richter, Laura Wischnewski, Jana Hölscher (Alfred Wegener Institute) and Arnold van Dijk (Utrecht University) for technical support. **[SS]**

## References


Badger, M.R., Price, G.D., 1989. Carbonic anhydrase activity associated with the cyanobacterium *Synechococcus* PCC7942. Plant Physiol. 89 (1), 51–60.

Badger, M.R., Palmqvist, K., Yu, J.W., 1994. Measurement of $CO_2$ and $HCO_3^-$ fluxes in cyanobacteria and microalgae during steady-state photosynthesis. Physiol. Plant. 90 (3), 529–536.

Badger, M.R., Andrews, T.J., Whitney, S.M., Ludwig, M., Yellowlees, D.C., Leggat, W., Price, G.D., 1998. The diversity and coevolution of RubisCO, plastids, pyrenoids, and chloroplast-based $CO_2$-concentrating mechanisms in algae. Can. J. Bot. 76 (6), 1052–1071.

Boller, A.J., Thomas, P.J., Cavanaugh, C.M., Scott, K.M., 2011. Low stable carbon isotope fractionation by coccolithophore RubisCO. Geochim. Cosmochim. Acta 75 (22), 7200–7207.

Burkhardt, S., Riebesell, U., Zondervan, I., 1999. Effects of growth rate, $CO_2$ concentration, and cell size on the stable carbon isotope fractionation in marine phytoplankton. Geochim. Cosmochim. Acta 63, 3729–3741.

Burkhardt, S., Amoroso, G., Riebesell, U., Sültemeyer, D., 2001. $CO_2$ and $HCO_3^-$ uptake in marine diatoms acclimated to different $CO_2$ concentrations. Limnol. Oceanogr. 46 (6), 1378–1391.

Cassar, N., Laws, E.A., Popp, B.N., 2006. Carbon isotopic fractionation by the marine diatom *Phaeodactylum tricornutum* under nutrient- and light-limited growth conditions. Geochim. Cosmochim. Acta 70 (21), 5323–5335.

Degens, E.T., Behrendt, M., Gotthardt, B., Reppmann, E., 1968. Metabolic fractionation of carbon isotopes in marine plankton—II. Data on samples collected off the coasts of Peru and Ecuador. Deep Sea Res. Oceanogr. Abstr. 15 (1), 11–20.

Eberlein, T., Van de Waal, D.B., Rost, B., 2014. Differential effects of ocean acidification on carbon acquisition in two bloom-forming dinoflagellate species. Physiol. Plant. http://dx.doi.org/10.1111/ppl.12137.

Eichner, M., Thoms, S., Kranz, S.A., Rost, B., 2015. Cellular inorganic carbon fluxes in *Trichodesmium*: a combined approach using measurements and modelling. J. Exp. Bot. 66 (3), 749–759.

Guillard, R.R.L., Ryther, J.H., 1962. Studies of marine planktonic diatoms. I. *Cyclotella nana* Hustedt and *Detonula confervacea* (Cleve) Gran. Can. J. Microbiol. 8, 229–239.

Guy, R.D., Fogel, M.L., Berry, J.A., 1993. Photosynthetic fractionation of the stable isotopes of oxygen and carbon. Plant Physiol. 101 (1), 37–47.

Hansen, P.J., Lundholm, N., Rost, B., 2007. Growth limitation in marine red-tide dinoflagellates: effects of pH versus inorganic carbon availability. Mar. Ecol. Prog. Ser. 334, 63–71.

Hinga, K.R., Arthur, M.A., Pilson, M.E., Whitaker, D., 1994. Carbon isotope fractionation by marine phytoplankton in culture: the effects of CO2 concentration, pH, temperature, and species. Glob. Biogeochem. Cyc. 8, 91–102.

Hoins, M., Van de Waal, D.B., Eberlein, T., Reichart, G.-J., Rost, B., Sluijs, A., 2015. Stable carbon isotope fractionation of organic cyst-forming dinoflagellates: evaluating the potential for a $CO_2$ proxy. Geochim. Cosmochim. Acta 160, 267–276.

Jasper, J.P., Hayes, J.M., 1990. A carbon isotope record of $CO_2$ levels during the late quaternary. Nature 347 (6292), 462–464.

John, U., Litaker, R.W., Montresor, M., Murray, S., Brosnahan, M.L., Anderson, D.M., 2014. Formal revision of the *Alexandrium tamarense* species complex (*Dinophyceae*) taxonomy: the introduction of five species with emphasis on molecular-based (rDNA) classification. Protist 165, 779–804.

Keller, M.D., Selvin, R.C., Claus, W., Guillard, R.R.L., 1987. Media for the culture of oceanic ultraplankton. J. Phycol. 23, 633–638.

Kottmeier, D.M., Rokitta, S.D., Tortell, P.D., Rost, B., 2014. Strong shift from $HCO_3^-$ to $CO_2$ uptake in *Emiliania huxleyi* with acidification: new approach unravels acclimation versus short-term pH effects. Photosynth. Res. 121 (2–3), 265–275.

Kottmeier, D.M., Rokitta, S.D., Rost, B., 2016. Acidification, not carbonation, is the major regulator of carbon fluxes in the coccolithophore *Emiliania huxleyi*. New Phytol. http://dx.doi.org/10.1111/nph.13885.

Kranz, S.A., Eichner, M., Rost, B., 2011. Interactions between CCM and $N_2$ fixation in *Trichodesmium*. Photosynth. Res. 109 (1–3), 73–84.

McNevin, D.B., Badger, M.R., Kane, H.J., Farquhar, G.D., 2006. Measurement of (carbon) kinetic isotope effect by Rayleigh fractionation using membrane inlet mass spectrometry for $CO_2$-consuming reactions. Funct. Plant Biol. 33 (12), 1115–1128.

Mook, W.G., Bommerson, J.C., Staverman, W.H., 1974. Carbon isotope fractionation between dissolved bicarbonate and gaseous carbon dioxide. Earth Planet. Sci. Lett. 22, 169–176.

Pagani, M., 2014. Biomarker-based inferences of past climate: the alkenone $pCO_2$ proxy. Treatise on Geochemistry, second ed.

Pierrot, D., Lewis, E., Wallace, D.W.R., 2006. MS excel program developed for $CO_2$ system calculations. ORNL/CDIAC-105a. Carbon Dioxide Information Analysis Center, Oak Ridge National Laboratory, US Department of Energy, Oak Ridge, Tennessee.

Price, G.D., Badger, M.R., Woodger, F.J., Long, B.M., 2008. Advances in understanding the cyanobacterial $CO_2$-concentrating-mechanism (CCM): functional components, $C_i$ transporters, diversity, genetic regulation and prospects for engineering into plants. J. Exp. Bot. 59 (7), 1441–1461.

Ratti, S., Giordano, M., Morse, D., 2007. $CO_2$-concentrating mechanisms of the potentially toxic dinoflagellate *Protoceratium reticulatum* (*Dinophyceae*, *Gonyaulacales*). J. Phycol. 43 (4), 693–701.

Raven, J.A., Johnston, A.M., 1991. Mechanisms of inorganic-carbon acquisition in marine phytoplankton and their implications for the use of other resources. Limnol. Oceanogr. 36, 1701–1714.

Roeske, C.A., O'Leary, M.H., 1984. Carbon isotope effects on enzyme-catalyzed carboxylation of ribulose bisphosphate. Biochemistry 23 (25), 6275–6284.

Rost, B., Zondervan, I., Riebesell, U., 2002. Light dependent carbon isotope fractionation in the coccolithophorid *Emiliania huxleyi*. Limnol. Oceanogr. 47, 120–128.

Rost, B., Riebesell, U., Burkhardt, S., Sültemeyer, D., 2003. Carbon acquisition of bloom-forming marine phytoplankton. Limnol. Oceanogr. 48 (1), 55–67.

Rost, B., Richter, K.-U., Riebesell, U., Hansen, P.J., 2006. Inorganic carbon acquisition in red tide dinoflagellates. Plant Cell Environ. 29, 810–822.

Rost, B., Kranz, S.A., Richter, K.-U., Tortell, P.D., 2007. Isotope disequilibrium and mass spectrometric studies of inorganic carbon acquisition by phytoplankton. Limnol. Oceanogr. Methods 5 (10), 328–337.

Schulz, K.G., Riebesell, U., Rost, B., Thoms, S., Zeebe, R.E., 2006. Determination of the rate constants for the carbon dioxide to bicarbonate interconversion in pH-buffered seawater systems. Mar. Chem. 100, 53–65.

Schulz, K.G., Rost, B., Burkhardt, S., Riebesell, U., Thoms, S., Wolf-Gladrow, D.A., 2007. The effect of iron availability on the regulation of inorganic carbon acquisition in the coccolithophore *Emiliania huxleyi* and the significance of cellular compartmentation for stable carbon isotope fractionation. Geochim. Cosmochim. Acta 71 (22), 5301–5312.

Scott, K.M., Henn-Sax, M., Harmer, T.L., Longo, D.L., Frame, C.H., Cavanaugh, C.M., 2007. Kinetic isotope effect and biochemical characterization of form IA RubisCO from the marine cyanobacterium *Prochlorococcus marinus* MIT9313. Limnol. Oceanogr. 52 (5), 2199–2204.

Sharkey, T.D., Berry, J.A., 1985. Carbon isotope fractionation of algae as influenced by an inducible $CO_2$ concentrating mechanism. In: Lucas, W.J., Berry, J.A. (Eds.), Inorganic Carbon Uptake by Aquatic Photosynthetic Organisms. The American Society of Plant Physiologists (ASPP), pp. 389–401.

Silvermann, D.N., 1982. Carbonic anhydrase. Oxygen-18 exchange catalyzed by an enzyme with rate-contributing proton-transfer steps. Methods Enzymol. 87, 732–752.

Trimborn, S., Wolf-Gladrow, D., Richter, K.U., Rost, B., 2009. The effect of $pCO_2$ on carbon acquisition and intracellular assimilation in four marine diatoms. J. Exp. Mar. Biol. Ecol. 376 (1), 26–36.

Van de Waal, D.B., John, U., Ziveri, P., Reichart, G.J., Hoins, M., Sluijs, A., Rost, B., 2013. Ocean acidification reduces growth and calcification in a marine dinoflagellate. PLoS One 8.

Whitney, S.M., Andrews, T.J., 1998. The $CO_2/O_2$ specificity of single subunit ribulose bisphosphate carboxylase from the dinoflagellate *Amphidinium carterae*. Aust. J. Plant Physiol. 25, 131–138.

Zeebe, R.E., Wolf-Gladrow, D.A., 2001. $CO_2$ in Seawater: Equilibrium, Kinetics, Isotopes. Elsevier Science, Amsterdam, The Netherlands.

# Update

Journal of Experimental Marine Biology and Ecology
Volume 503, Issue , June 2018, Page 147

DOI: https://doi.org/10.1016/j.jembe.2018.02.003

Journal of Experimental Marine Biology and Ecology 503 (2018) 147

Contents lists available at ScienceDirect

Journal of Experimental Marine Biology and Ecology

journal homepage: www.elsevier.com/locate/jembe

Corrigendum

# Corrigendum to "CO2-dependent carbon isotope fractionation in dinoflagellates relates to their inorganic carbon fluxes" [J. Exp. Mar. Biol. Ecol. 481 (2016) 9–14]

Mirja Hoins[a,b,*], Tim Eberlein[b], Dedmer B. Van deWaal[c], Appy Sluijs[a,*], Gert-Jan Reichart[a,d], Björn Rost[b]

[a] Department of Earth Sciences, Faculty of Geosciences, Utrecht University, Budapestlaan 4, 3584, CD, Utrecht, The Netherlands
[b] Marine Biogeosciences, AlfredWegener Institute, Helmholtz Centre for Polar- and Marine Research, Am Handelshafen 12, 27570 Bremerhaven, Germany
[c] Department of Aquatic Ecology, Netherlands Institute of Ecology (NIOO-KNAW), Droevendaalsesteeg 10, 6708 PBWageningen, The Netherlands
[d] Royal Netherlands Institute for Sea Research (NIOZ), Landsdiep 4, 1797 SZ 't Horntje, Texel, The Netherlands

In the original article Fig. 1 was incorrect, which has now been amended. The authors would like to apologise for any inconvenience caused.

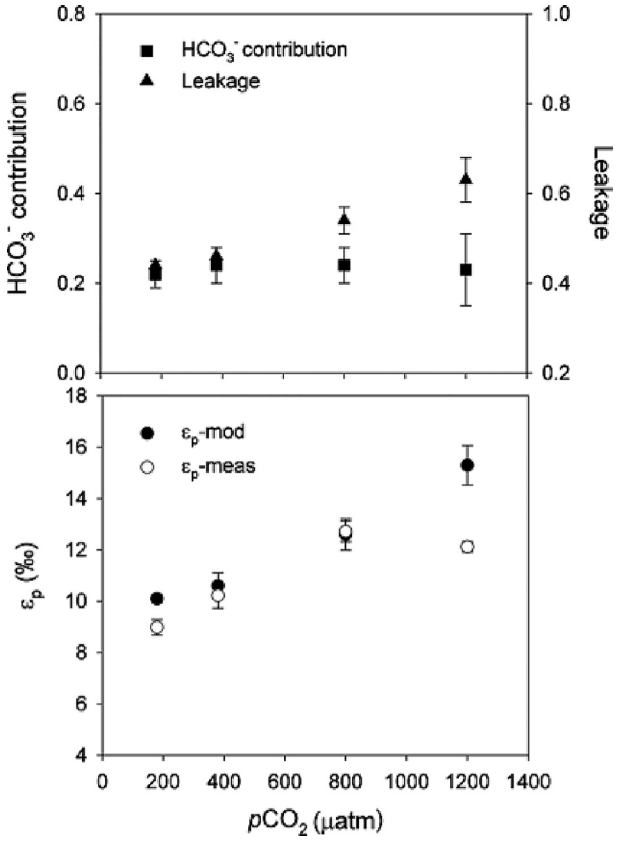


DOI of original article: http://dx.doi.org/10.1016/j.jembe.2016.04.001
* Corresponding authors at: Department of Earth Sciences, Faculty of Geosciences, Utrecht University, Budapestlaan 4, 3584, CD, Utrecht, The Netherlands.
*E-mail addresses:* mhoins@awi.de (M. Hoins), a.sluijs@uu.nl (A. Sluijs).

https://doi.org/10.1016/j.jembe.2018.02.003

Available online 26 February 2018
0022-0981/